



Published in final edited form as:

*Science*. 2016 April 22; 352(6284): aaf0659. doi:10.1126/science.aaf0659.

## Detyrosinated microtubules buckle and bear load in contracting cardiomyocytes

Patrick Robison<sup>1</sup>, Matthew A. Caporizzo<sup>2</sup>, Hossein Ahmadzadeh<sup>2</sup>, Alexey I. Bogush<sup>1</sup>, Christina Yingxian Chen<sup>1</sup>, Kenneth B. Margulies<sup>3</sup>, Vivek B. Shenoy<sup>2</sup>, and Benjamin L. Prosser<sup>1,\*</sup>

<sup>1</sup>Department of Physiology, Pennsylvania Muscle Institute, University of Pennsylvania Perelman School of Medicine, Philadelphia, PA 19104, USA

<sup>2</sup>Department of Materials Science and Engineering, University of Pennsylvania School of Engineering and Applied Science, Philadelphia, PA 19104, USA

<sup>3</sup>Department of Medicine, University of Pennsylvania Perelman School of Medicine, Philadelphia, PA 19104, USA

### Abstract

**INTRODUCTION**—Along with its well-documented role as a track for cargo transport, the microtubule (MT) cytoskeleton is linked to diverse structural and signaling roles in the cardiac myocyte. MTs can facilitate the rapid transmission of mechanical signals to intracellular effectors, a process termed mechanotransduction. A proliferated MT network may also provide a mechanical resistance to cardiac contraction in certain disease states. Yet our understanding of how MTs resist compression and transmit mechanical signals has been impaired by a lack of direct observation and by the unpredictable effects of blunt pharmacological tools.

**RATIONALE**—Direct observation of MT mechanical behavior during contraction is the most straightforward way to elucidate the mechanisms underlying MT contributions to heart function. Advances in imaging have made this possible at temporal and spatial resolutions that permit quantification of MT geometry during the contraction cycle. Furthermore, recent evidence suggests that posttranslational modification of the microtubule network, specifically “detyrosination,” regulates cardiac mechanotransduction. This raises the question of whether detyrosination alters how microtubules respond to the changing mechanical loads inherent to each cardiac cycle. To answer these questions, we used advanced imaging techniques to explore MT behavior in beating murine cardiomyocytes.

---

\*Corresponding author. bpros@mail.med.upenn.edu.

#### SUPPLEMENTARY MATERIALS

[www.sciencemag.org/content/352/6284/aaf0659/suppl/DC1](http://www.sciencemag.org/content/352/6284/aaf0659/suppl/DC1)

Materials and Methods

Supplementary Text

Figs. S1 to S11

Tables S1 to S9

References (35–42)

Movies S1 to S8

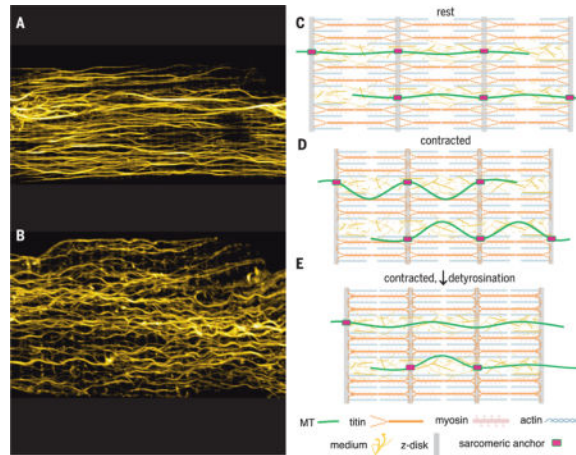
**RESULTS**—During contraction, MTs must somehow accommodate the changing geometry of the myocyte. In a typical myocyte, this was accomplished by deforming into a sinusoidal buckled configuration that returned to an identical resting configuration after each beat. The periodic nature of these buckles coincided with the repeating contractile units of the cardiomyocyte known as sarcomeres, which suggested a direct interaction. Desmin intermediate filaments were identified as a key component of an anchoring complex that links MTs to the sarcomere and imparts structural organization to the MT network.

The physical link between microtubules and the sarcomere was highly dependent on detyrosination. In myocytes where detyrosination was suppressed, MTs often accommodated the contraction by sliding past each other rather than buckling as the sarcomere shortened. Disrupting the MT-sarcomere interaction allowed the sarcomere to shorten farther and faster, as well as decreased overall stiffness. Conversely, promoting detyrosination was sufficient to increase myocyte stiffness and impede the contraction of the myocyte. Consistently, clinical data showed a direct correlation between excess detyrosination and functional decline in patients with hypertrophic cardiomyopathy.

**CONCLUSION**—Thus, microtubules can provide mechanical resistance to the myocyte through interactions with the sarcomere, forming load-bearing spring elements in parallel with the contractile apparatus. These interactions are mediated by a detyrosination-dependent association with desmin that regulates myocyte stiffness and contractility. Excess detyrosination promotes the interaction between MTs and the sarcomere, which increases resistance to contraction and may contribute to reductions in cardiac function in certain disease states.

**Graphical abstract**

**MTs in the beating heart.** When a cardiomyocyte (A) is compressed (B), as occurs during systolic contraction, MTs buckle under load. In a typical myocyte (C), detyrosinated MTs are mechanically coupled to the sarcomere and buckle during contraction (D). When detyrosination is reduced (E), this interaction is disrupted and MTs buckle less, which allows sarcomeres to shorten and stretch with less resistance.



Along with its well-defined transport functions, the microtubule (MT) network serves multiple mechanical roles in the beating cardiomyocyte. MTs function as

mechanotransducers, converting changing contractile forces into intracellular signals (1, 2). MTs may also act as compression-resistant elements, which could provide a mechanical impediment to cardiomyocyte contraction (3–5). If so, they must bear some of the compressive and tensile load of a working myocyte. Unfortunately, little is known about MT behavior during the contractile cycle. During this cycle, Ca<sup>2+</sup>-mediated actin-myosin interaction first shortens repeating contractile units called sarcomeres, which are then stretched as the heart fills with blood during diastole.

Although an isolated MT would present minimal resistance to myocyte compression, the stiffness of the network within a living cell, with MT-associated proteins and other cytoskeletal elements, can change by orders of magnitude (6, 7). It is in this context that MTs are proposed to act as compression-resistant elements (6, 8) that may impair sarcomere shortening and thus cardiac function, particularly in disease states associated with MT proliferation (8–10). Posttranslational modification (PTM) of MTs (11, 12) could also modify their mechanical properties and binding interactions. Detyrosination, a PTM of  $\alpha$ -tubulin, has recently been shown to augment MT-dependent mechanotransduction in dystrophic cardiac and skeletal muscle (12). This specific PTM is also increased in animal models of heart disease (1, 13, 14), which raises a mechanistic question: If mechano-signaling is altered, have the mechanical properties of the myocyte changed?

Although the idea that a proliferated (and perhaps modified) MT network may mechanically interfere with contraction is attractive, the “MT hypothesis” has remained controversial [for reviews, see (15, 16)]. Two important limitations have hindered our understanding: (i) a reliance on blunt pharmacological tools (colchicine/Taxol) that have off-target consequences; (ii) a lack of direct observation of MTs under the stress and strain of the contractile cycle. Here, we characterized MTs under contractile loads using a high-resolution imaging technique and directly tested how MT detyrosination may regulate load-bearing and the mechanical properties of the myocyte.

## MTs buckle under contractile load

MT networks in cardiomyocytes have two major features (Fig. 1A): an orthogonal grid just beneath the membrane that wraps the myofibrils and a deeper network composed primarily of longitudinal elements that interdigitate the myofibrils. Longitudinal MTs often run many sarcomeres in length but do not span the full cell. Given that cardiomyocytes change shape during contraction, the MT cytoskeleton must accommodate this change. There are three apparent possibilities: MTs not anchored to other cytoskeletal or sarcomeric proteins could rearrange or slide passively with the surrounding medium; anchored MTs could directly experience contractile force and themselves deform under load; or the MTs could break and/or disassemble and reform. These possibilities offer divergent mechanisms for the regulation of mechano-signaling and the overall mechanics of the myocyte. Without direct observation, however, this behavior has been difficult to quantify.

Standard confocal imaging, although capable of resolving MTs in living cells (17), suffers from limitations in the signal-to-noise ratio when pushed to speeds that can resolve events on the time scale of cardiomyocyte contraction (Fig. 1B and movie S1). Consequently, we

turned to a high-speed, subdiffraction limit technique called Airyscan (see fig. S1). This technology maintains high signal-to-noise ratios at the required temporal resolution, while offering a 1.7-fold improvement in spatial resolution beyond the standard diffraction limit.

Using the MT-binding fluorogenic dye SiR tubulin, based on the fluorophore silicon rhodamine (18) (Fig. 1C and movie S2), we imaged internal MTs during contractions triggered by a 1 Hz electrical field stimulation in isolated mouse cardiomyocytes. We were able to capture MT behavior during contraction and found that longitudinally oriented MTs frequently deformed and developed sinusoidal buckles. Because SiR tubulin may polymerize MTs (18), we also generated adenovirus encoding a small fragment of the MT-binding protein ensconsin fused to three copies of GFP (EMTB-3xGFP) to decorate MTs. We achieved similar results (table S1) but with improved signal-to-noise ratios (Fig. 1D and movie S3).

We measured blindly selected MTs for deformation with two parameters—amplitude and wavelength (Fig. 1G). Where possible, the same MT was followed through contraction. Amplitude rose quickly from resting to contracted levels (Fig. 1H), with clearly visible buckles. Using a threshold of two standard deviations above resting amplitude, we found that two-thirds of MTs buckle under control conditions (Fig. 1H).

MT buckles quickly reversed during relaxation, and the configuration of the MT network between contractions tightly colocalized with the network configuration from previous cycles (Fig. 1, E and F), with a minimal mean reduction in Pearson's colocalization of 0.01 per contractile cycle ( $n = 18$  runs). The rapid and precise reversibility of the network deformations suggested tight coupling to the contractile apparatus, and it argues against MT breakage and regrowth contributing to mechanical properties and signaling over the time scale of myocyte contraction.

A notable feature of the MT buckles was the emergence of subpopulations of buckle wavelength centered at  $\sim 1.65 \mu\text{m}$ ,  $3.3 \mu\text{m}$ , and perhaps even  $4.7 \mu\text{m}$  (Fig. 1I). These corresponded closely to the length of one, two, or three contracted sarcomeres, respectively. Although MTs buckling outside of these populations could be found in our data without difficulty, these subpopulations were strongly indicative of ordered geometric constraints on the buckling MT. This was observed in certain cells where faint transverse staining at the Z-disc shows MTs buckling between sarcomeric constraints (movie S4).

## Detyrosination regulates MT buckling in the heart

This robust buckling behavior of the MT network may be a result of a particularly high abundance of “detyrosinated” MTs in adult cardiomyocytes (19). Detyrosination is a PTM of  $\alpha$ -tubulin where the C-terminal tyrosine residue has been cleaved by a tubulin carboxypeptidase (TCP); this process can be readily reversed by tubulin tyrosine ligase (TTL) (11). This tyrosination cycle is evolutionarily conserved across eukaryotes (20) and appears required for life (21), yet its functional roles are still poorly understood. Because detyrosination can protect MTs from disassembly (22, 23) and can facilitate their cross-linking with intermediate filaments (IFs) (24, 25), we hypothesized that the high proportion

of detyrosination may confer the resilient load-bearing capabilities of the cardiac cytoskeletal network.

Using antibodies specific to detyrosinated  $\alpha$ -tubulin, we found a high abundance of detyrosination in the  $\alpha$ -tubulin network of adult myocytes (Fig. 2, A and B), as expected (12, 19). To test the role of detyrosinated MTs, we generated adenovirus encoding TTL (AdV-TTL) with a *Discosoma* red fluorescent protein (DsRed) reporter. Expressing this construct in isolated cardiomyocytes could effectively reduce the level of detyrosination as shown by both immunofluorescence (Fig. 2, A and B) and immunoblot (Fig. 2, C and D), which resulted in a 71% reduction in the amount of polymerized, detyrosinated MTs, with a concomitant up-regulation of tyrosinated tubulin (Fig. 2, C and D, and fig. S2). Overexpression of TTL also resulted in a modest (10%) reduction in the density of the polymerized MT network (Fig. 2B), consistent with an increased disassembly of tyrosinated MTs (22, 23). We complemented this genetic strategy with a pharmacological approach to inhibit TCP using parthenolide (PTL) (26). PTL treatment also reduced the fraction of detyrosinated MTs, albeit to a lesser extent (42%) than AdV-TTL and with no effect on MT network density (fig. S2).

The load-bearing behavior of the MT network in cardiomyocytes overexpressing TTL or treated with PTL was dramatically different from control myocytes. Tyrosinated MTs frequently seemed to simply slide in the moving cell (Fig. 2, E and F, orange arrows; movies S5 and S6; and fig. S3), rather than buckling under load. This behavior was again reversible, with a minimum reduction in Pearson's colocalization over successive contractions that was not different from controls ( $P = 0.87$ ,  $n = 19$  runs). The occurrence of buckling in TTL-overexpressing and PTL-treated cells fell significantly (Fig. 2G, left), whereas amplitude changes observed on the same MT between rest and contraction also dropped significantly (Fig. 2G, right, and table S1).

When MT buckling was observed, the mean wavelength was not significantly different between control and TTL-overexpressing cells (table S1). However, the majority of MTs in TTL-overexpressing myocytes no longer buckled at the wavelength of a single sarcomere, and no subpopulations at multiples of the sarcomeric period were observed (Fig. 2H). Instead, the majority of these MTs buckled in a single population at wavelengths between 2 and 3  $\mu\text{m}$ , which suggested that MT buckling was less constrained by a sarcomeric interaction after detyrosination was reduced (Fig. 2I).

## Detyrosinated MTs resist contractile compression

The energy required to deform detyrosinated MTs under compressive load could confer some meaningful resistance to myocyte contraction. We thus tested directly if MT detyrosination affects contractility in beating cardiomyocytes. After overexpression of TTL, we found significant enhancements in both the magnitude (Fig. 3, A to C) and peak rate (Fig. 3, D and E) of sarcomere shortening (table S2). PTL had a similar effect on contractility (Fig. 3F and table S2). Peak relaxation rates were also increased, which could be because of a decrease in cellular viscosity (see below) or may reflect the increased magnitude of shortening and, therefore, compression of internal elastic elements (e.g., titin)

that develop restoring force (27). These contractile changes were not associated with any significant difference in global calcium transients (Fig. 3, G to I) or resting sarcomere length (Fig. 3C), which suggested a change in intrinsic mechanical resistance associated with the ability of detyrosinated MTs to bear compressive load.

## Detyrosination regulates myocyte mechanical properties

We next measured mechanical resistance directly using atomic force microscopy (AFM). AFM measurements of transverse stiffness were performed across a range of indentation rates. Myocyte stiffness changed substantially with indentation rate and was well fit by a standard linear solid model (SLSM) [methods in supplementary materials (SM)] (fig. S4 and Fig. 4A). At low rates (100 nm/s), the stiffness of the cardiomyocyte was essentially elastic, reported as E1, and was reduced by PTL treatment and TTL overexpression (Fig. 4B). At higher rates, the modulus increased by E2, which reflects cross-linked material inside the cell that slips on the time scale of slower measurements but “turns on” (stiffens) at faster time scales ( $> 2 \mu\text{m/s}$ ) (28). The viscosity derived by the SLSM defines the rate above which these cross-links are engaged. TTL overexpression significantly decreased E2 and viscosity (Fig. 4B), which suggested that reducing detyrosination decreases the number of cross-links engaged at physiological strain rates in the cardiomyocyte.

The fact that MTs deform under load and resist sarcomere shortening implies a transfer of force between MTs and the sarcomere. If MTs resist longitudinal compression, they could also confer a tensile resistance when the sarcomeres are stretched, as occurs during diastolic filling. To test this idea, we measured passive stiffness directly along the longitudinal axis of TTL-overexpressing myocytes. We attached cardiomyocytes to laser-etched cell holders (Fig. 4C, fig. S5, and movie S7) via a biological adhesive (1) and subjected them to steplike changes in length, while simultaneously measuring sarcomere length and passive force with a high-sensitivity transducer (Fig. 4D). A typical force response (Fig. 4D, blue) showed a rapid rise to peak force during the high-velocity stretch ( $F_{\text{peak}}$ ), containing both elastic and viscous elements, followed by a relaxation to a steady-state force ( $F_{\text{s.s.}}$ ) that largely reflects the elastic stiffness of the myocyte. For a given step size, TTL-overexpressing myocytes exerted significantly reduced peak forces during physiological length changes, with modest reductions in steady-state force (fig. S5F). The TTL-overexpressing cells also underwent significantly larger changes in sarcomere length with any given step (fig. S5G), which indicated increased sarcomere compliance and which suggested that stiffer sarcomeres in control cells distribute the length change to other compliant components in series. As can be surmised from fig. S5, F and G, TTL overexpression decreased tension across the physiological range of sarcomere lengths achieved during diastolic filling (Fig. 4E), which indicated a role for detyrosinated MTs as tensile-resistant elements. Visual evidence supporting such a relation was seen in MT networks in a control cell at resting and stretched length (fig. S5 and Fig. 4C, cyan). At resting length, there was some inherent slack in the MT network, whereas the same MTs became taut when the cell was stretched and held at long sarcomere lengths (movie S8).

## Model of MT contribution to cardiac contractility

We next sought to develop a mathematical model to recapitulate the experimentally measured changes in MT buckling and contractility when detyrosination is reduced. Previous work modeling MT buckles (6) suggests that three critical variables determine buckling behavior; MT stiffness, stiffness of the surrounding medium, and force incident on the long axis of the MT. How these three variables are predicted to alter MT behavior and myocyte mechanics is described in fig. S6. Of the three, only a decrease in incident force can explain our experimental observations after suppressing detyrosination. If MT anchoring to the sarcomere is disrupted, the reduced incident force on the MT may drop below the critical force required for buckling, which results in simultaneous decreases in buckling amplitude (Fig. 2) and viscoelasticity (Figs. 3 and 4). The sarcomeric periodicity of buckles (Fig. 1I) also suggests an underlying structural constraint that changes in MT or medium stiffness alone cannot explain. We thus chose to model MT buckling within a contractile model that includes a MT compression-resistive element that's interaction with the sarcomere can be varied (see model in SM for details).

Using the mechanical scheme detailed in Fig. 5A, we fitted the contraction resulting from a log-normal force input to derive both contractile and buckling parameters. By modifying the incident force applied to a MT for a given amount of sarcomere shortening (Fig. 5A and model in SM), we simulated the effect of a sarcomeric anchor sliding and then catching at detyrosinated regions of the MT. Inclusion of a 100-nm slide (50 nm at each anchor, see model) before MTs engage with the rest of the sarcomere is reasonable, given the ~80% reduction in detyrosinated area observed by immunofluorescence with TTL overexpression (Fig. 2C), and reflects the fact that reductions in detyrosination would increase the average distance between detyrosinated tubulins that could interact strongly with MT anchoring points. This disruption of MT-sarcomere coupling produced model outputs (Fig. 5, C and D) that closely recapitulated our experimental contractility and buckling results.

An alternate possibility to the sliding anchor is that the anchor is completely uncoupled by suppressing detyrosination and reverts to buckling behavior governed by local viscoelasticity rather than underlying structure, as proposed for less rigidly organized cell types, including developing myocytes (6). In either case, the coupling of MTs to the sarcomere is reduced, which impairs their ability to resist contraction.

## Potential role for desmin as a sarcomeric MT anchor

The putative characteristics of the anchor—a mechanically stiff protein capable of forming complexes with MTs and restricted to a spatially defined region of the sarcomere—suggested the intermediate filament desmin as an immediate candidate. Desmin forms structural bundles that form a complex with the Z-disc (29), and intermediate filaments can form detyrosination-dependent cross-links with MTs (30, 31).

We first sought to determine whether desmin preferentially associates with detyrosinated MTs. Cosedimentation of cardiomyocyte lysates showed that desmin forms pellets with polymerized MTs (Fig. 6A) in direct proportion to their level of detyrosination (Fig. 6, B

and C), which indicated a specific and sensitive interaction. We also co-stained cardiomyocytes from desmin-depleted [knockout (KO)] and wild-type (WT) mice for desmin and both tyrosinated and detyrosinated tubulin to observe any preferential interaction. The two populations of MTs show similar overall patterning in WT myocytes, except for a specific accumulation of detyrosinated (and not tyrosinated) tubulin in transverse bands at the Z-disc that colocalized with desmin (Fig. 6, D and E, and fig. S7). Note that KO animals lacked this transverse pattern completely (Fig. 6D and fig. S7H), although the Z-disc itself remained intact (fig. S7C). In addition, KO myocytes had a denser (fig. S7F) and more disorganized MT network (Fig. 6D and fig. S7, B and E), which suggested that desmin is required for proper MT network organization.

If desmin cross-links with detyrosinated MTs to structurally reinforce the network, then the removal of desmin should both decrease cytoskeletal stiffness and prevent tyrosination-dependent changes in viscoelasticity. Blind studies in WT and KO myocytes revealed that desmin KO myocytes were significantly less stiff than WT counterparts (Fig. 6, F and G), and that treatment with PTL no longer reduced viscoelasticity (Fig. 6, F and G).

### MT detyrosination is sufficient to impair cardiomyocyte contractility

Increasing detyrosination correlates with impaired function in animal models of heart disease (13, 14). Thus, we next tested whether increasing detyrosination could directly impair cardiac contractility. Using an adenoviral construct expressing short hairpin RNAs (shRNAs) against TTL (shTTL), we suppressed TTL expression, which enhanced detyrosination (Fig. 7A and fig. S8). shTTL-transduced myocytes were then tested for their viscoelastic and contractile properties. The excess detyrosination alone was sufficient to increase viscosity and stiffness (Fig. 7, B and C) and suppressed contractile velocity and magnitude (Fig. 7, D and E).

We next examined whether this modification correlated with functional deficits in human heart disease. To this end, we analyzed left ventricular tissue samples from healthy patient donors and from patients exhibiting varying degrees of heart disease due to several underlying causes (table S7). Detyrosinated tubulin was significantly increased in patients with clinically diagnosed hypertrophic and dilated cardiomyopathies (HCM and DCM, respectively), along with a modest increase in total tubulin content (Fig. 7, F and G). Blind analysis of HCM patient data showed that detyrosination inversely correlated with left ventricular ejection fraction (LVEF), a primary indicator of cardiac contractility (Fig. 7H). There was no such correlation detected between LVEF and total or tyrosinated tubulin levels, nor any correlation between heart weight and detyrosination (fig. S9), which suggested a specific link between detyrosination and LVEF. Myocardium from patients with DCM all demonstrated considerably depressed LVEF and variable, but increased, detyrosinated tubulin.

TTL was unchanged in all patient populations, which showed that a decreased expression of the tyrosinating enzyme does not explain the increase in detyrosinated tubulin in patients with heart disease (Fig. 7G). Because the molecular identity of TCP is unknown, it is unclear if up-regulation of the detyrosinating enzyme may underlie this effect.



## Discussion

Our findings demonstrate a regulatory pathway for MT load-bearing and myocyte mechanics through posttranslational detyrosination of tubulin. Detyrosinated MTs buckle under load in contracting cardiomyocytes, which confers mechanical resistance to contraction and regulating the viscoelastic properties of the myocyte.

The observation that MTs normally buckle, rather than break or slide, strongly indicates that they bear load and store elastic bending energy during the cardiac contractile cycle. This has implications for MT-dependent mechano-signaling in muscle and other tissues (1, 32, 33) but also has direct implications for contractility. Our model of myocyte contractility demonstrates how changing MT load-bearing and force transfer with the sarcomeres can substantially alter contractile properties. Our experimental data show that such changes in MT load-bearing can be achieved by posttranslational modifications of the MTs themselves, particularly detyrosination. The measured reductions in buckling and viscoelasticity and the increase in contractile speed of PTL-treated, TTL-overexpressing myocytes can all be attributed to changing the way MTs interact with the sarcomere and impairing their ability to act as compression resistors. It is also possible that detyrosinated MTs anchored to one sarcomere form bundles with MTs anchored to adjacent sarcomeres. If so, disrupting bundling would also effectively uncouple MTs from force-generating structures. Regardless of the mechanism, disrupting coupling to sarcomeres would reduce the incident force on the MT, and buckling occurrence would drop.

The striking periodicity of buckles in untreated myocytes lends further support to the idea of a sarcomeric anchor. The preferential association of desmin with detyrosinated tubulin and the insensitivity of desmin KO animals to changes in detyrosination strongly implicates desmin as at least one component of a sarcomeric anchoring complex of detyrosinated MTs. Note that myocytes lacking desmin have decreased viscoelasticity, despite a denser MT network, which supports the idea that MT network organization and cross-linking is a stronger determinant of myocyte mechanical properties than network density per se. Both the desmin and MT networks have elements perpendicular to their typical orientation, particularly near the sarcolemma, which may alter how those elements interact with the cytoskeleton and plasma membrane. However, we believe that the preponderance of the contractile resistance that results from detyrosination is due to longitudinal MTs in an orthogonal grid with transverse desmin IFs because of the simple numerical majority of cytoskeletal elements in this configuration.

Despite the fact that detyrosinated MTs store energy during sarcomere contraction, which provides compression resistance, little of this energy appears to return in the form of a restoring force that would quicken sarcomere extension. This implies that energy used to deform MTs undergoes substantial loss. Buckling of the MT exerts compressive force on the surrounding matrix and deforms the cytoplasm, which, due to its intrinsic viscosity, can act as an energy sink during each cycle. This is reflected in the large viscous component of the MT contributions to myocyte mechanical properties observed at deformation rates consistent with contractile velocities both in this and previous work (34). However, we do note a slight prolongation of the late phase of relaxation in TTL-overexpressing myocytes, which may

represent the loss of a MT contribution to restoring force. We consider it probable that the restoring force of other internal elastic elements, such as titin, are likely to play a more dominant role, at least in the initial return toward resting sarcomere length (27). Thus, an increase in detyrosination may increase myocyte stiffness and impair contraction by acting as an energy sink, without providing significant energetic return during relaxation.

Consistent with this, an increase in detyrosination was associated with clinical contractile dysfunction in human hearts. Our cellular studies demonstrate that acute reduction of detyrosination with genetic or pharmacologic approaches can boost contractility and reduce mechanical stiffness. Additionally, these approaches are able to induce large changes in detyrosination, while only slightly altering the overall MT cytoskeleton, which minimizes off-target consequences. Thus, interfering with detyrosination may represent an attractive and novel therapeutic strategy for increasing contractility.

In conclusion, our data show that MTs exhibit divergent mechanical behavior because of the differences in how they couple to the rest of the cardiac cytoskeleton. The tyrosinated portions of the network, moving readily with the myocyte during contraction, provide little contractile resistance. Conversely, the detyrosinated portions of the MT network, forming complexes with desmin IFs, produce a cross-linked MT-IF network that confers robust resistance to contraction. This orthogonal MT-IF grid requires tightly periodic MT deformations to accommodate myocyte morphology changes during contraction. These deformations require a considerable amount of energy to form and dissipate a large fraction of that energy due to viscous interactions. This has important implications for MT load-bearing across cell biology, as well as for the altered mechanical stiffness and mechano-signaling in cardiac disease.

## Supplementary Material

Refer to Web version on PubMed Central for supplementary material.

## Acknowledgments

The authors thank C. W. Ward and E. L. Holzbaur for kindly providing TTL and EMTB-3xGFP plasmids, respectively, as well as for discussion; R. Bloch for providing desmin KO mice and littermate controls; Carl Zeiss Microscopy for Airyscan instrumentation use; IonOptix for technical support and cell holder materials; and Y. E. Goldman, E. L. Grishchuk, and R. J. Composto for discussion and guidance. B.L.P., P.R., M.A.C., A.I.B., and K.B.M. were responsible for experimental design; B.L.P., P.R., M.A.C., C.Y.C., and A.I.B. carried out experiments and analyzed data; H.A. and V.B.S. designed and executed the mathematical model. B.L.P. and P.R. cowrote the manuscript. All authors participated in the critical review and revision of the manuscript. This work was supported by funding from National Institute for Arthritis and Musculoskeletal and Skin Diseases (NIH) (T32AR053461-09 to P.R. and T32HL007954 to M.A.C.) and from National Heart, Lung, and Blood Institute (NIH) (R00-HL114879 to B.L.P.). The VIVA experiments used shared experimental facilities from the Nano Science and Engineering Center on Molecular Function at the Nano-Bio Interface at the University of Pennsylvania supported by NSF under grant DMR08-32802. We thank R. Composto, who acknowledges the NSF Polymers Program under grant DMR09-07493. Procurement of human heart tissue was enabled by grants from NIH (HL089847 and HL105993) to K.B.M. H.A. and V.B.S. are supported by the National Institute of Biomedical Imaging and Bioengineering (NIH) under award number R01EB017753 and NSF grant CMMI-1312392. The data are included in the main manuscript and in the supplementary materials online.

## REFERENCES AND NOTES

1. Prosser BL, Ward CW, Lederer WJ. X-ROS signaling: Rapid mechano-chemo transduction in heart. *Science*. 2011; 333:1440–1445. DOI: 10.1126/science.1202768 [PubMed: 21903813]
2. Prosser BL, Ward CW, Lederer WJ. X-ROS signaling is enhanced and graded by cyclic cardiomyocyte stretch. *Cardiovasc Res*. 2013; 98:307–314. DOI: 10.1093/cvr/cvt066 [PubMed: 23524301]
3. Zile MR, et al. Constitutive properties of adult mammalian cardiac muscle cells. *Circulation*. 1998; 98:567–579. DOI: 10.1161/01.CIR.98.6.567 [PubMed: 9714115]
4. Nishimura S, et al. Microtubules modulate the stiffness of cardiomyocytes against shear stress. *Circ Res*. 2006; 98:81–87. DOI: 10.1161/01.RES.0000197785.51819.e8 [PubMed: 16306445]
5. Granzier HL, Irving TC. Passive tension in cardiac muscle: Contribution of collagen, titin, microtubules, and intermediate filaments. *Biophys J*. 1995; 68:1027–1044. DOI: 10.1016/S0006-34959580278-X [PubMed: 7756523]
6. Brangwynne CP, et al. Microtubules can bear enhanced compressive loads in living cells because of lateral reinforcement. *J Cell Biol*. 2006; 173:733–741. DOI: 10.1083/jcb.200601060 [PubMed: 16754957]
7. Mehrbod M, Mofrad MRK. On the significance of microtubule flexural behavior in cytoskeletal mechanics. *PLOS ONE*. 2011; 6:e25627.doi: 10.1371/journal.pone.0025627 [PubMed: 21998675]
8. Tsutsui H, Ishihara K, Cooper G 4th. Cytoskeletal role in the contractile dysfunction of hypertrophied myocardium. *Science*. 1993; 260:682–687. DOI: 10.1126/science.8097594 [PubMed: 8097594]
9. Zile MR, et al. Role of microtubules in the contractile dysfunction of hypertrophied myocardium. *J Am Coll Cardiol*. 1999; 33:250–260. DOI: 10.1016/S0735-10979800550-6 [PubMed: 9935038]
10. Cooper G 4th. Cytoskeletal networks and the regulation of cardiac contractility: Microtubules, hypertrophy, and cardiac dysfunction. *Am J Physiol Heart Circ Physiol*. 2006; 291:H1003–H1014. DOI: 10.1152/ajpheart.00132.2006 [PubMed: 16679401]
11. Janke C, Bulinski JC. Post-translational regulation of the microtubule cytoskeleton: Mechanisms and functions. *Nat Rev Mol Cell Biol*. 2011; 12:773–786. DOI: 10.1038/nrm3227 [PubMed: 22086369]
12. Kerr JP, et al. Detyrosinated microtubules modulate mechanotransduction in heart and skeletal muscle. *Nat Commun*. 2015; 6:8526.doi: 10.1038/ncomms9526 [PubMed: 26446751]
13. Sato H, et al. Microtubule stabilization in pressure overload cardiac hypertrophy. *J Cell Biol*. 1997; 139:963–973. DOI: 10.1083/jcb.139.4.963 [PubMed: 9362514]
14. Belmadani S, Poüs C, Ventura-Clapier R, Fischmeister R, Méry P-F. Post-translational modifications of cardiac tubulin during chronic heart failure in the rat. *Mol Cell Biochem*. 2002; 237:39–46. DOI: 10.1023/A:1016554104209 [PubMed: 12236585]
15. White E. Mechanical modulation of cardiac microtubules. *Pflugers Arch*. 2011; 462:177–184. DOI: 10.1007/s00424-011-0963-0 [PubMed: 21487691]
16. Cooper G 4th. Cardiocyte cytoskeleton in hypertrophied myocardium. *Heart Fail Rev*. 2000; 5:187–201. DOI: 10.1023/A:1009836918377 [PubMed: 16228904]
17. Cassimeris L, Tran P. *Methods Cell Biol*. 2010; 97:xvii–xviii. DOI: 10.1016/S0091-679X1097031-3 [PubMed: 20719261]
18. Lukinavičius G, et al. Fluorogenic probes for live-cell imaging of the cytoskeleton. *Nat Methods*. 2014; 11:731–733. DOI: 10.1038/nmeth.2972 [PubMed: 24859753]
19. Belmadani S, Poüs C, Fischmeister R, Méry P-F. Post-translational modifications of tubulin and microtubule stability in adult rat ventricular myocytes and immortalized HL-1 cardiomyocytes. *Mol Cell Biochem*. 2004; 258:35–48. DOI: 10.1023/B:MCBI.0000012834.43990.b6 [PubMed: 15030168]
20. Janke C, et al. Tubulin polyglutamylase enzymes are members of the TTL domain protein family. *Science*. 2005; 308:1758–1762. DOI: 10.1126/science.1113010 [PubMed: 15890843]
21. Erck C, et al. A vital role of tubulin-tyrosine-ligase for neuronal organization. *Proc Natl Acad Sci USA*. 2005; 102:7853–7858. DOI: 10.1073/pnas.0409626102 [PubMed: 15899979]

22. Peris L, et al. Motor-dependent microtubule disassembly driven by tubulin tyrosination. *J Cell Biol.* 2009; 185:1159–1166. DOI: 10.1083/jcb.200902142 [PubMed: 19564401]
23. Sirajuddin M, Rice LM, Vale RD. Regulation of microtubule motors by tubulin isotypes and post-translational modifications. *Nat Cell Biol.* 2014; 16:335–344. DOI: 10.1038/ncb2920 [PubMed: 24633327]
24. Kreitzer G, Liao G, Gundersen GG. Detyrosination of tubulin regulates the interaction of intermediate filaments with microtubules in vivo via a kinesin-dependent mechanism. *Mol Biol Cell.* 1999; 10:1105–1118. DOI: 10.1091/mbc.10.4.1105 [PubMed: 10198060]
25. Whipple RA, et al. Vimentin filaments support extension of tubulin-based microtentacles in detached breast tumor cells. *Cancer Res.* 2008; 68:5678–5688. DOI: 10.1158/0008-5472.CAN-07-6589 [PubMed: 18632620]
26. Fonrose X, et al. Parthenolide inhibits tubulin carboxypeptidase activity. *Cancer Res.* 2007; 67:3371–3378. DOI: 10.1158/0008-5472.CAN-06-3732 [PubMed: 17409447]
27. Helmes M, Trombitás K, Granzier H. Titin develops restoring force in rat cardiac myocytes. *Circ Res.* 1996; 79:619–626. DOI: 10.1161/01.RES.79.3.619 [PubMed: 8781495]
28. Mahaffy RE, Shih CK, MacKintosh FC, Käs J. Scanning probe-based frequency-dependent microrheology of polymer gels and biological cells. *Phys Rev Lett.* 2000; 85:880–883. DOI: 10.1103/PhysRevLett.85.880 [PubMed: 10991422]
29. Konieczny P, et al. Myofiber integrity depends on desmin network targeting to Z-disks and costameres via distinct plectin isoforms. *J Cell Biol.* 2008; 181:667–681. DOI: 10.1083/jcb.200711058 [PubMed: 18490514]
30. Liao G, Gundersen GG. Kinesin is a candidate for cross-bridging microtubules and intermediate filaments. Selective binding of kinesin to detyrosinated tubulin and vimentin. *J Biol Chem.* 1998; 273:9797–9803. DOI: 10.1074/jbc.273.16.9797 [PubMed: 9545318]
31. Gurland G, Gundersen GG. Stable, detyrosinated microtubules function to localize vimentin intermediate filaments in fibroblasts. *J Cell Biol.* 1995; 131:1275–1290. DOI: 10.1083/jcb.131.5.1275 [PubMed: 8522589]
32. Khairallah RJ, et al. Microtubules underlie dysfunction in duchenne muscular dystrophy. *Sci Signal.* 2012; 5:ra56.doi: 10.1126/scisignal.2002829 [PubMed: 22871609]
33. Prager-Khoutorsky M, Khoutorsky A, Bourque CW. Unique interweaved microtubule scaffold mediates osmosensory transduction via physical interaction with TRPV1. *Neuron.* 2014; 83:866–878. DOI: 10.1016/j.neuron.2014.07.023 [PubMed: 25123313]
34. Tagawa H, et al. Cytoskeletal mechanics in pressure-overload cardiac hypertrophy. *Circ Res.* 1997; 80:281–289. DOI: 10.1161/01.RES.80.2.281 [PubMed: 9012750]

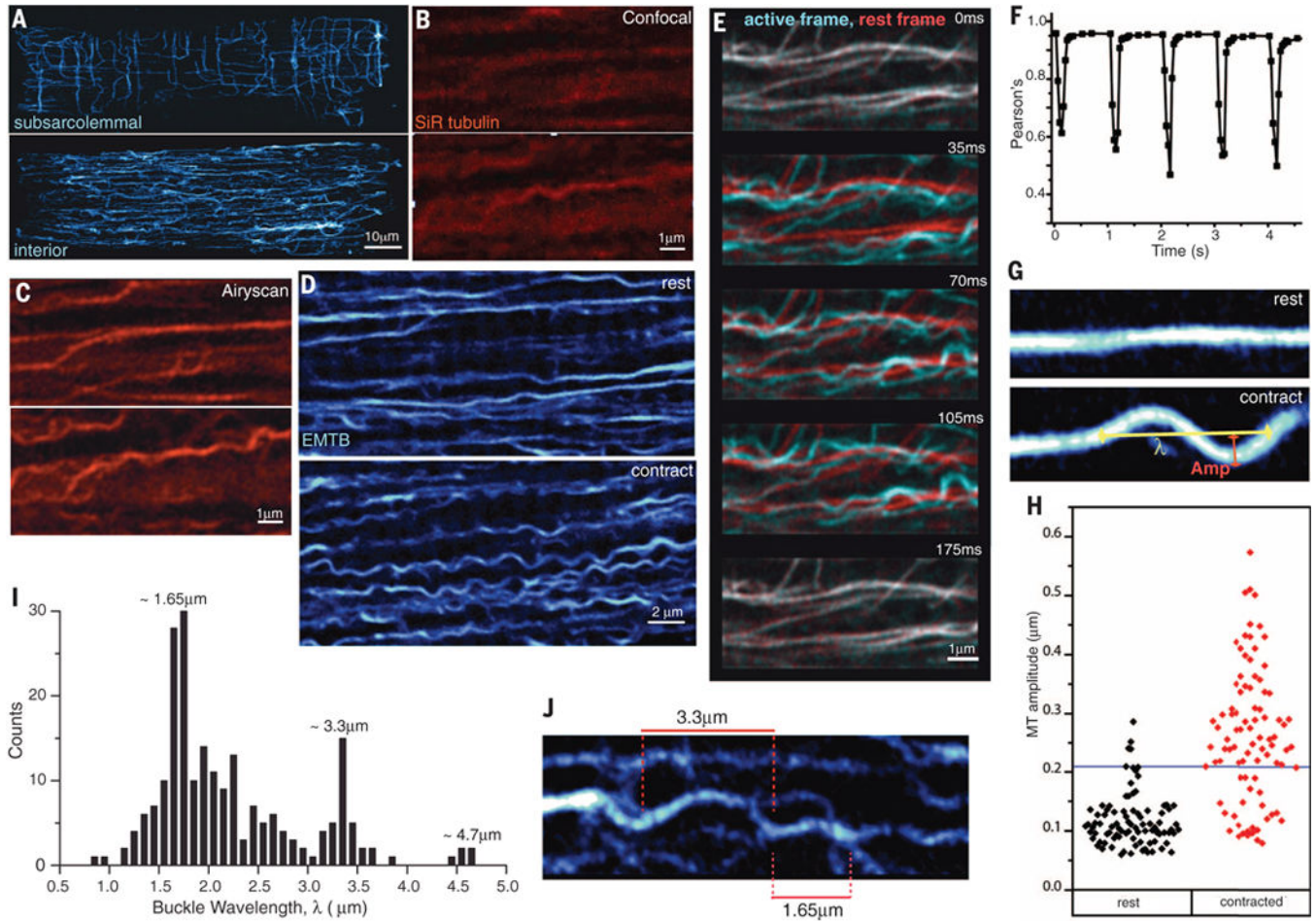


**Fig. 1. MTs reversibly buckle in contracting cardiomyocytes**

(A) The subsurface (top) and interior (bottom) cardiomyocyte MT network. (B) High-speed confocal imaging of MTs at rest (top) and during contraction (bottom) labeled with SiR tubulin with brightness increased for comparison with (C). (C) Airyscan imaging of the same MTs as in (B) at rest and during contraction. (D) Wider view of MTs labeled with EMTB-3xGFP at rest (top) and during contraction (bottom). (E) MTs imaged throughout a contractile cycle (cyan) were overlaid onto the network configuration from the initial frame at rest (red). (F) Colocalization analysis of (E) shows that MTs repeatedly return to the same position. Pearson's coefficient is used to estimate goodness of fit to original MT configuration over several contractile cycles. Initial drop to  $\sim 0.96$  is due to imaging noise. (G) Quantification of buckling amplitude (measured from centerline to edge) and  $\lambda$  (wavelength measured as twice the distance between consecutive inflection points). (H) Amplitude of MTs labeled with EMTB-3xGFP in resting (black) and contracted (red) cardiomyocytes. The threshold to determine buckling occurrence (blue line) was two standard deviations above the mean resting value. (I) Distribution of buckling wavelengths in cardiomyocytes shows a dominant population between 1.6 and 1.7  $\mu\text{m}$ , and a second population at 3.3  $\mu\text{m}$ . (J) A representative MT demonstrating buckles with wavelengths that correspond to the distance between one (1.65  $\mu\text{m}$ ) or two (3.3  $\mu\text{m}$ ) adjacent sarcomeres.

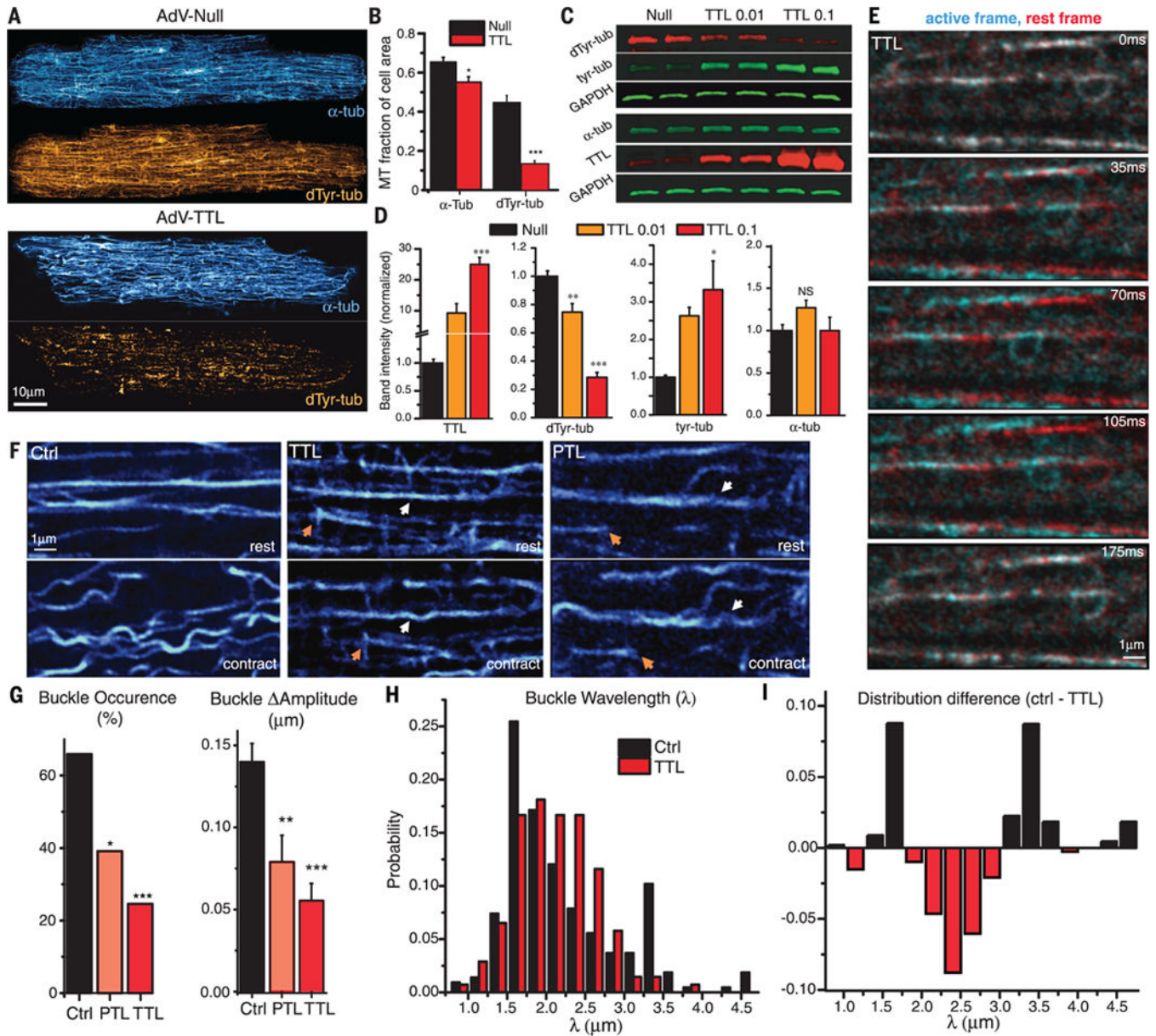


**Fig. 2. Detyrosination underlies MT buckling**

(A) The MT cytoskeleton (blue and aqua) in rat adult cardiomyocytes (top) is heavily detyrosinated (orange). TTL overexpression (bottom) reduces detyrosination dramatically but makes comparatively small changes in the overall MT network. (B) Quantification of the fraction of cell area covered by  $\alpha$ -tubulin and detyrosinated tubulin (dTyr-tubulin) in null ( $n = 14$ ) and TTL-overexpressing ( $n = 13$ ) cells, as determined from thresholded images as shown in fig. S2E. (C and D) Western blots from cardiomyocyte lysates show the effects of viral overexpression of TTL. GAPDH, glyceraldehyde-3-phosphate dehydrogenase. (E) Time course of MTs in a contracting cardiomyocyte (cyan) transduced with AdV-TTL overlaid on the resting MT configuration (red). MTs appear to translocate along the contractile axis rather than deforming. (F) Comparison of MTs in resting (top) and contracted (bottom) cardiomyocytes in control, TTL, and PTL groups. In TTL and PTL

groups, some MTs slide (orange arrows) relative to others that deform (white arrows). Additional examples are provided in fig. S3. **(G)** Buckling occurrence and amplitude are reduced by overexpression of TTL or treatment with PTL. **(H)** Buckling wavelength distribution in control and TTL-overexpressing myocytes and **(I)** the difference between these distributions. Overexpression of TTL causes MTs to buckle more often at wavelengths between 2 and 3  $\mu\text{m}$ , and MTs are far less likely to buckle at distinct sarcomeric wavelengths (1.7 and 3.3  $\mu\text{m}$ ) when detyrosination is reduced. Data are presented as means  $\pm$  SEM; \* $P < 0.05$ , \*\* $P < 0.01$ , \*\*\* $P < 0.001$ . Further statistical details are available in table S1.

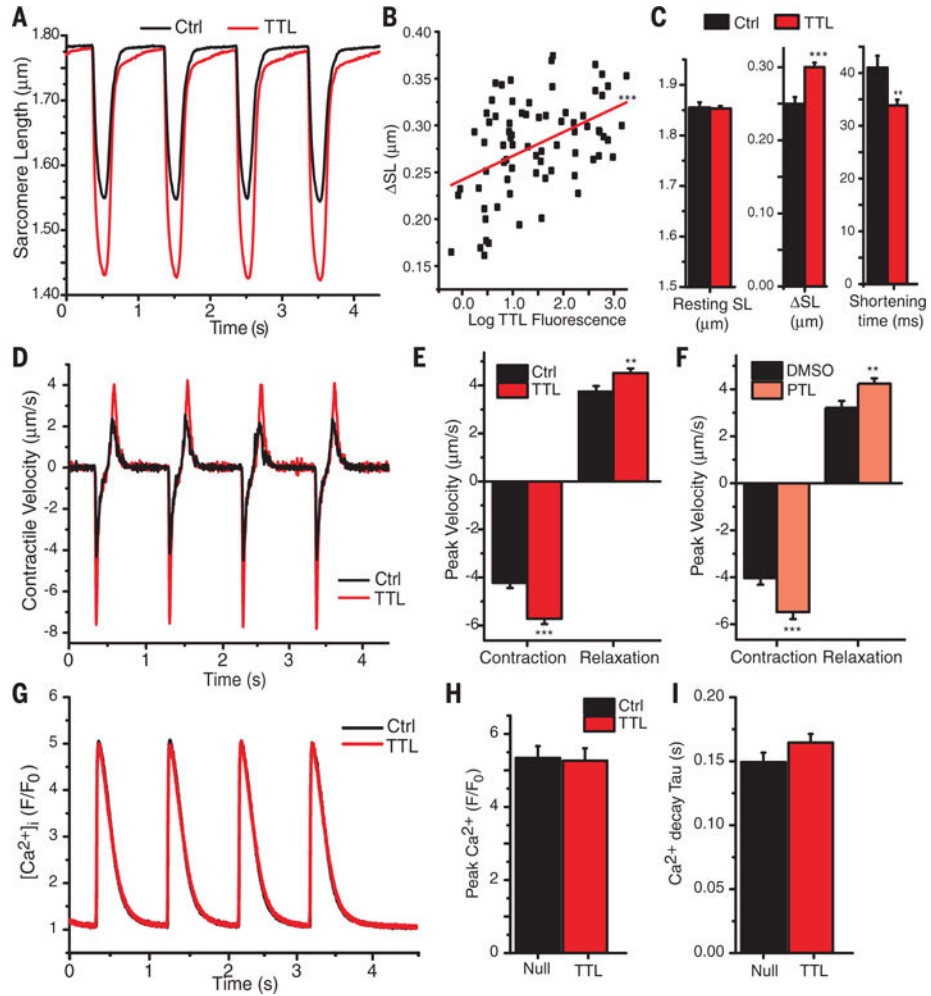


**Fig. 3. Detyrosinated MTs impede contractility**

(A) Sarcomere shortening (DSL) during contraction is increased in TTL-overexpressing myocytes. This change is (B) dose-dependent [ $P = 1.2 \times 10^{-5}$ , correlation coefficient ( $r^2$ ) = 0.23] and (C) associated with a faster shortening time without affecting resting sarcomere length. (D) First derivative of traces in (A) demonstrate contractile velocities in control and TTL-overexpressing myocytes. (E) TTL-overexpressing myocytes demonstrate an increase in the peak velocity of both contraction and relaxation. (F) PTL-treated cells display similar behavior. (G to I) Despite the significant changes in contractility, no changes in the peak or kinetics of the global calcium transient were observable.  $F/F_0$ , the change in fluorescence from the original fluorescence before stimulation. Data are presented as means  $\pm$  SEM; \* $P < 0.05$ , \*\* $P < 0.01$ , \*\*\* $P < 0.001$ . Further statistical details are available in table S2.



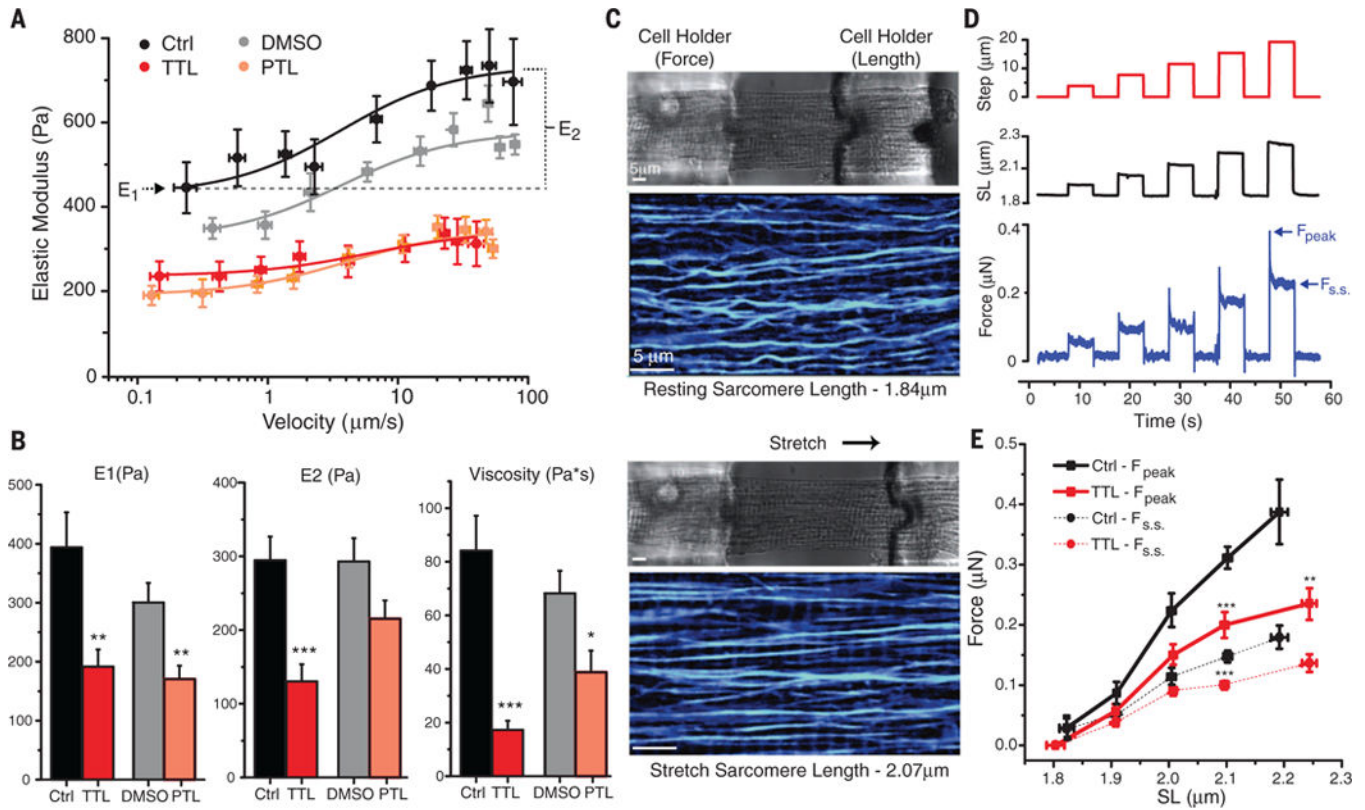


**Fig. 4. Detyrosinated MTs regulate the viscoelasticity of cardiomyocytes**

(A) Elastic modulus of cardiomyocytes measured by AFM at various indentation velocities and fit to SLSM (see methods in SM). (B) Quantification of velocity-independent (E1) and velocity-dependent (E2) components of the elastic modulus, and SLSM fit-derived viscosity. Both TTL overexpression and PTL treatment significantly reduced elasticity and viscosity. There were no significant differences in these parameters between dimethyl sulfoxide (DMSO) (gray) and AdV-null (black) transduced cells ( $P = 0.28, 0.34, \text{ and } 0.33$ , respectively). Reductions in stiffness due to TTL overexpression are also apparent in cells under stretch along the longitudinal axis. (C) Myocytes were attached via glass cell holders (C, top, and fig. S5) to a force transducer and length controller and were subjected to stretch. MTs visualized by EMTB-3xGFP (C, blue and aqua) at rest (top) and at a stretched length (bottom). (D) Representative force versus length protocol. A series of stepwise stretches (red) in 4- $\mu\text{m}$  increments are applied to an isolated myocyte, which increases sarcomere length (SL, black). Passive tension (blue) generated by the step relaxes quickly from a peak value to a new steady state. (E) Force measurements binned according to measured change in sarcomere length with a given step size. TTL-overexpressing cells exert reduced peak passive tension during step changes in length, with a more modest reduction in steady-state tension. Data are presented as means  $\pm$  SEM; \* $P < 0.05$ , \*\* $P < 0.01$ , \*\*\* $P < 0.001$ . Further statistical details are available in tables S3 and S4.

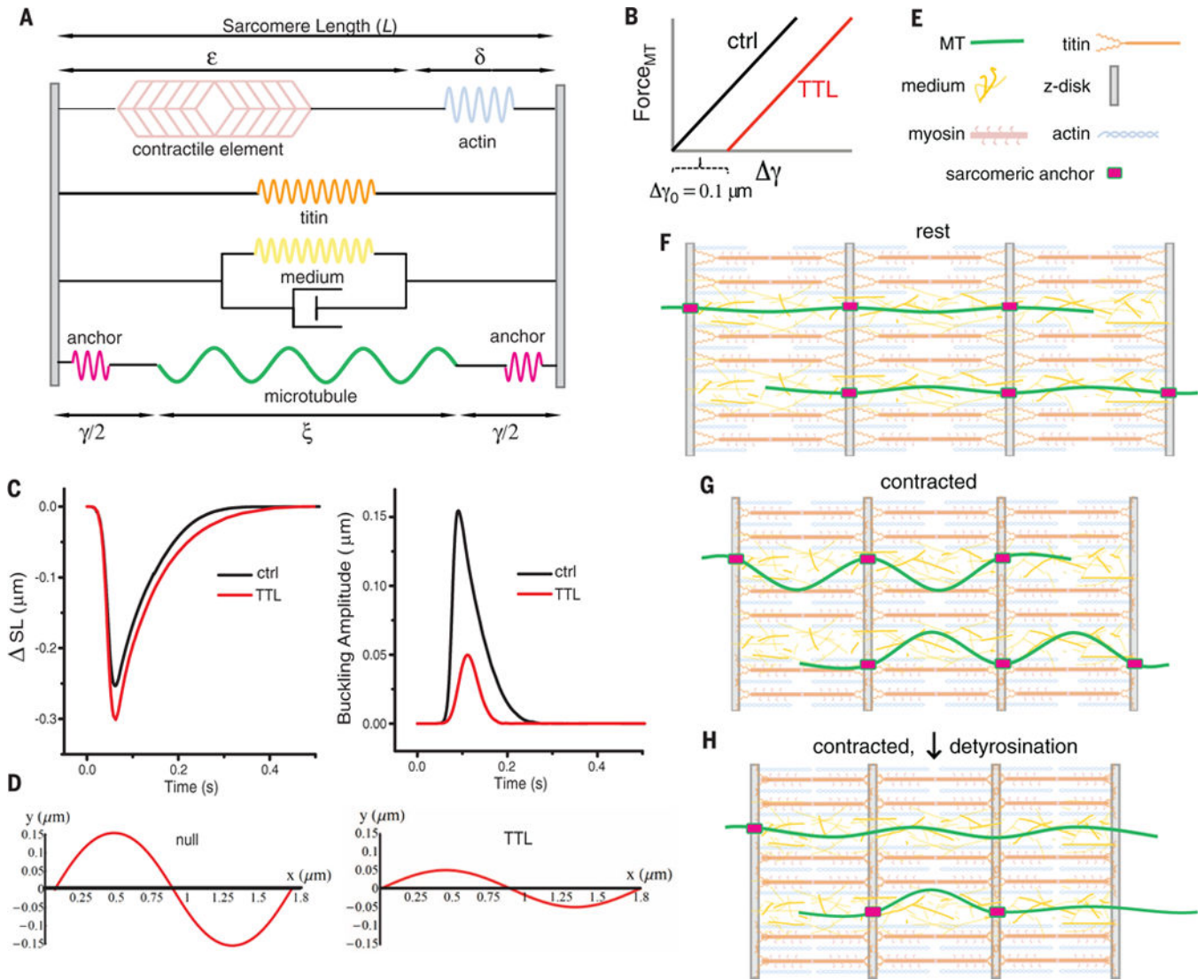


**Fig. 5. Modeling MTs in the contracting sarcomere**

(A) Mechanical schematic of the modeled sarcomere. A force-generating contractile arm (top) is coupled in parallel at the Z-disc to a spring element representing titin (orange), a viscoelastic medium (yellow spring and dashpot), and a MT (green) with anchors (fuschia pink) to the Z-disc (gray). The anchor to the Z-disc is only engaged at regions of MT detyrosination. (B) TTL overexpression is modeled by allowing the anchors to slide for 50 nm at each end before engaging and transmitting force to the MT at a detyrosinated subunit. (C) The change in sarcomere length at peak contraction and buckling amplitude. (C) and (D) recapitulate experimental observations for TTL-overexpressing myocytes after this change. (E and F) The cardiac sarcomere, shown with MTs with putative stiff anchors to the sarcomere, here, at the Z-disc. Contraction reduces the distance between anchor points, which requires the MTs either to buckle (G) if the anchors are engaged or to slide (H), if the anchors are not engaged and force incident on the MT remains low. Mathematical model parameters are available in table S5.

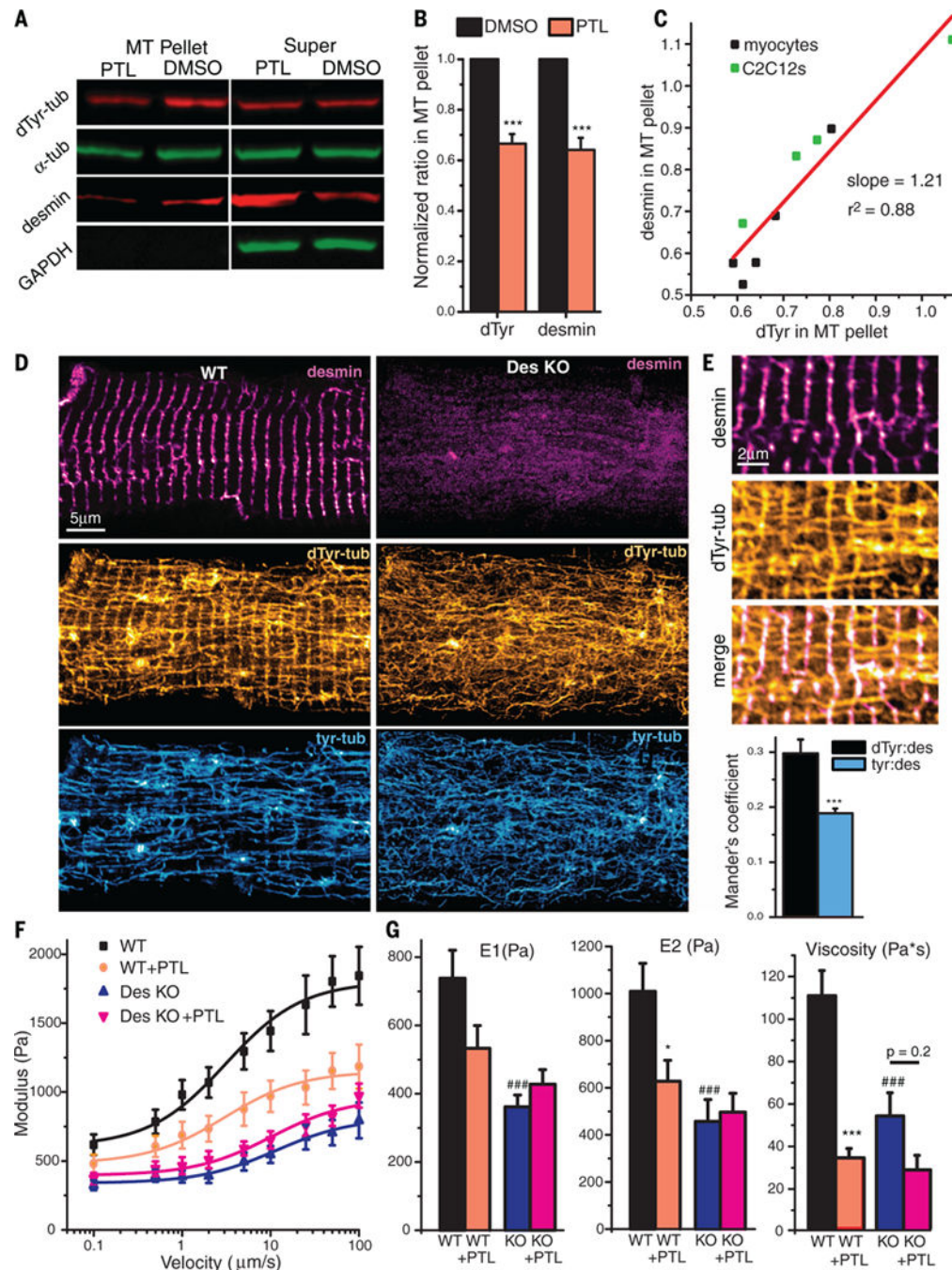


**Fig. 6. Desmin associates with detyrosinated MTs to increase cardiomyocyte stiffness**  
**(A)** MT cosedimentation shows the interaction between polymerized MTs (pellet) and desmin. **(B)** Quantification of the amount of detyrosination and desmin (relative to the total amount of tubulin) in the MT pellet from cardiomyocyte lysates with and without PTL treatment. Data were normalized to DMSO level. **(C)** The amount of desmin associated with the MTs after PTL treatment is directly proportional to the amount of MT detyrosination across several experiments in rat cardiomyocytes and C2C12 cells. **(D)** Immunofluorescence of desmin, dTyr, and Tyr-tubulin shows dTyr-specific transverse pattern in WT, but not

desmin KO, myocytes. **(E)** Overlay of dTyr-tubulin and desmin. (See fig. S7 for more examples.) **(F and G)** AFM measurements show a PTL-dependent reduction in myocyte stiffness and viscosity in WT, but not desmin, KO myocytes. Viscoelasticity in desmin KO myocytes is not statistically different from WT with PTL treatment. Data are presented as means  $\pm$  SEM; \* $P < 0.05$ , \*\* $P < 0.01$ , \*\*\* $P < 0.001$  with respect to DMSO treatment; ### $P < 0.001$  with respect to untreated WT myocytes. Further statistical details are available in table S6.

Author Manuscript

Author Manuscript

Author Manuscript

Author Manuscript

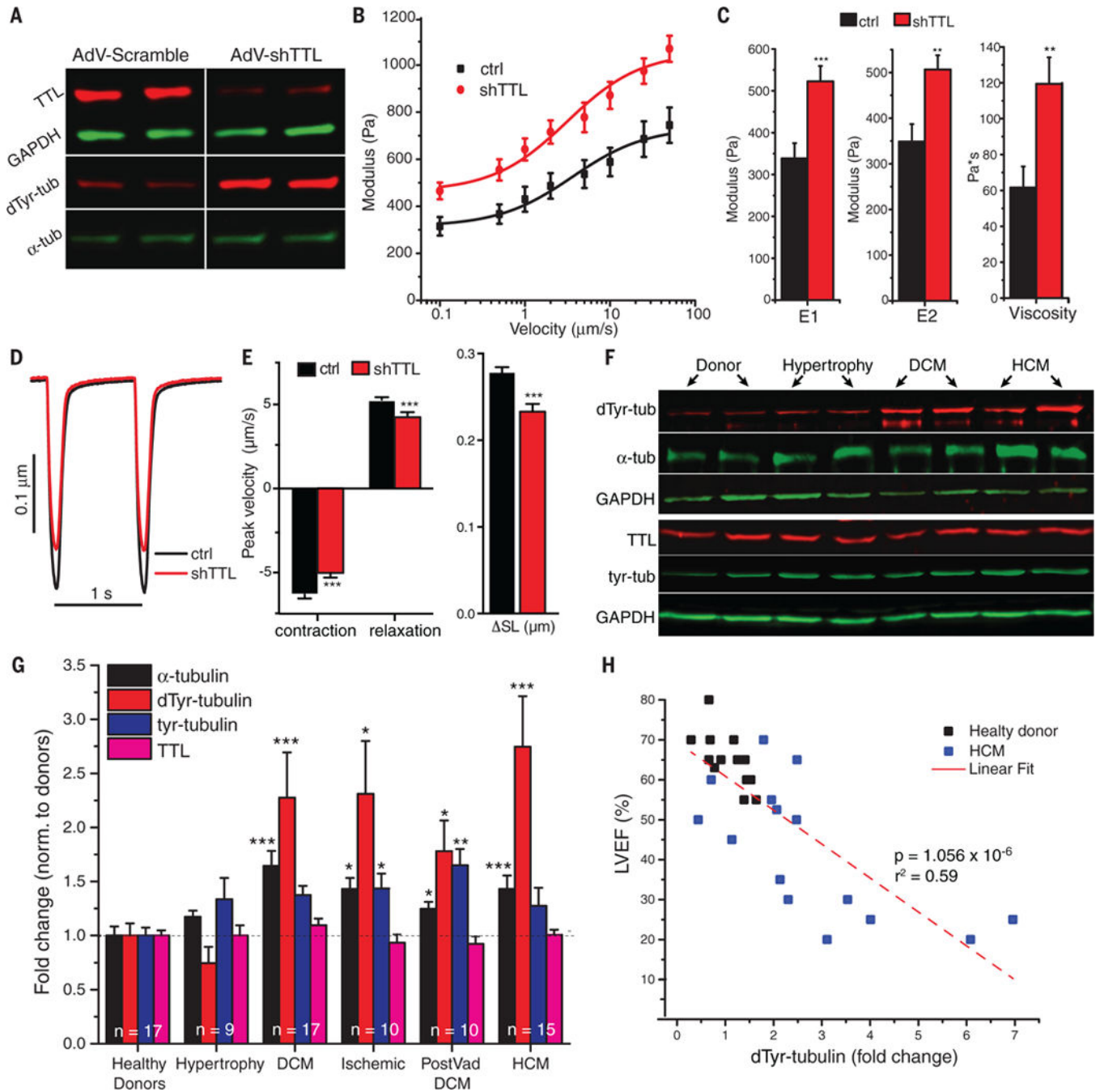


**Fig. 7. Increasing detyrosination impairs contraction and is associated with human heart failure** (A) Western blot shows that shRNA against TTL selectively increases dTyr-tubulin without changing overall levels of  $\alpha$ -tubulin. (B) Elastic modulus of control and shTTL-expressing myocytes at various indentation rates. (C) shTTL myocytes demonstrate increases in E1, E2, and viscosity. (D and E) TTL suppression significantly reduces contractile magnitude and velocity. (F) Representative Western blots from human heart lysates. (G) Data from pooled analysis;  $n = 17$  healthy donors, 9 hypertrophy, 17 DCM, 11 ischemic, 10 with DCM following ventricular assist device support (VAD DCM), and 15 HCM hearts. (H) There was

a negative correlation between LVEF and dTyr-tubulin expression in control and hypertrophic cardiomyopathy patients. Data are presented as means  $\pm$  SEM; \* $P < 0.05$ , \*\* $P < 0.01$ , \*\*\* $P < 0.001$ . Further statistical details are available in tables S7 to S9.

Author Manuscript

Author Manuscript

Author Manuscript

Author Manuscript